Skating on a Film of Air: Drops Impacting on a Surface

John M. Kolinski,[1] Shmuel M. Rubinstein,[1,2,*] Shreyas Mandre,[3] Michael P. Brenner,[1] David A. Weitz,[1,2] and L. Mahadevan[1,2]

[1]School of Engineering and Applied Sciences, Harvard University, Cambridge, Massachusetts 02138, USA
[2]Department of Physics, Harvard University, Cambridge, Massachusetts 02138, USA
[3]Division of Engineering, Brown University, 182 Hope Street, Providence, Rhode Island 02912, USA

(Received 23 September 2011; published 15 February 2012)

The commonly accepted description of drops impacting on a surface typically ignores the essential role of the air that is trapped between the impacting drop and the surface. Here we describe a new imaging modality that is sensitive to the behavior right at the surface. We show that a very thin film of air, only a few tens of nanometers thick, remains trapped between the falling drop and the surface as the drop spreads. The thin film of air serves to lubricate the drop enabling the fluid to skate on the air film laterally outward at surprisingly high velocities, consistent with theoretical predictions. Eventually this thin film of air breaks down as the fluid wets the surface via a spinodal-like mechanism. Our results show that the dynamics of impacting drops are much more complex than previously thought, with a rich array of unexpected phenomena that require rethinking classic paradigms.

DOI: 10.1103/PhysRevLett.108.074503 PACS numbers: 47.55.db, 47.20.Ky, 47.55.dr, 68.03.−g

Raindrops splashing on a car window, ink-jets printing on a sheet of paper, and the dripping faucet in the kitchen are all everyday experiences which depend on the impact of drops of fluid on a surface. As familiar as these phenomena are, the impact of a drop of fluid on a surface is, in fact, quite complex [1–5]. Particularly stunning are the beautiful splashing patterns that often occur [6,7]; our understanding of these is predicated on very rapid impact followed by a shock wave as the fluid bounces back from the surface [8,9]. However, before contact can occur, the drop must first drain the air separating it from the surface. Indeed, experimental studies showing the suppression of splashing at reduced ambient pressure underscore the importance of the air [1,10–13]. Recent theoretical calculations suggest that, even at moderate impact velocities, the air fails to drain and is instead compressed, deforming and flattening the bottom of the drop while serving as a thin cushion of air a few tens of nanometers thick to lubricate the spread of the drop [1,13], and leading to the eventual formation of a trapped bubble of air within the drop [14]. However, the initial stages of impact occur over diminutive length scales and fleeting time scales, and the very existence of this thin film of air remains controversial [15]; indeed, this film has never been directly observed. Moreover, the mechanisms leading the breakup of this film and the ultimate wetting of the surface have never even been considered. Testing these ideas requires direct observations of the impacting interface; however, this demands development of new experimental methods to attain the requisite spatial and temporal resolution.

In this Letter, we describe direct measurements of the initial contact dynamics of a drop impacting a dry glass surface. To visualize the impact we image from below rather than from the side; to discern the very thin film we combine total internal reflection (TIR) microscopy [16] with a novel virtual frame technique (VFT). We directly observe a thin film of air that initially separates the liquid from the surface enabling much more rapid lateral spreading of the drop providing striking confirmation of the theoretical predictions [1]. However, we also observe a complex sequence of events that leads to the rupture of the film and ultimate contact of the liquid with the solid surface; the initially smooth air film breaks up as discrete holes are formed and are filled by the liquid. These holes rapidly spread and coalesce into a ring of wet surface surrounding a trapped bubble of air.

To observe the thin film of air, we illuminate the top surface of an optically smooth dove prism (BK7 glass) with collimated light incident from below at an angle greater than the critical angle for total internal reflection at a glass-air interface but smaller than that at the glass-liquid interface. The reflected light is imaged with a fast camera, as shown schematically in Fig. 1(a). The light reflected from each point of the interface, $I_r(x, y)$, depends exponentially on the separation between the impacting fluid and the solid surface, with a characteristic decay length that depends on the angle of incidence and is of the order of 50 nm; as the separation decreases further the incident light is no longer fully totally internally reflecting and I_r decreases. This directly probes the thin film of air. We illustrate this using a 1.3-mm-radius isopropanol (IPA) drop falling from an initial height $H = 21$ cm, where H is the distance from the surface to the tip of the nozzle where the drop is generated. When the drop is far from the surface the illuminating beam is totally internally reflected and nothing is observed as shown in Fig. 1(b); we thus define the last frame before we observe a change in the image as $t = 0$. However, as the separation between the drop and the solid surface becomes

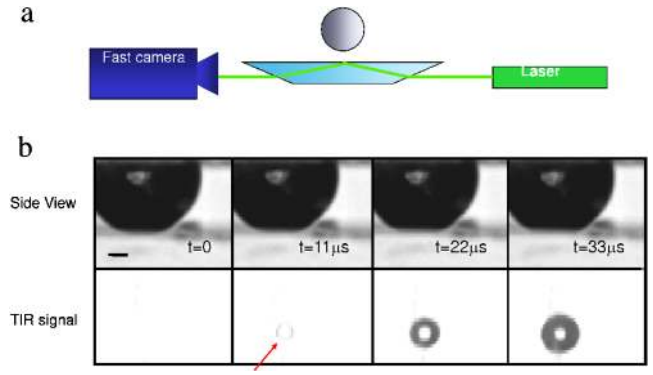

FIG. 1 (color online). Experimental setup. (a) Schematic of TIR microscopy. (b) Four typical images of a 2.6-mm-diameter drop, falling from $H = 21$ cm viewed simultaneously from the side and with TIR. Scale bar is 400 μm

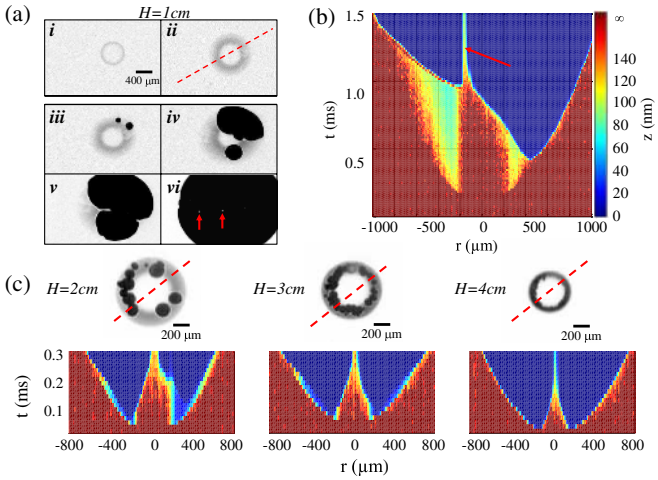

FIG. 2 (color online). The behavior of the thin air film separating the impacting drop from the surface. (a) Six TIR snapshots of a drop, released from $H = 1$ cm illustrating the film of air and the impact dynamics. The two bubbles remaining in the drop are indicated by the arrows in (vi). (b) The impact dynamics along the cut shown by the dashed line in (a)(ii). The height is indicated by the color. The arrow indicates one of the bubbles that remains trapped in the liquid. (c) The TIR images and time evolution of the air films along the dashed lines for $H = 2$, 3, and 4 cm. The exposure time for all snapshots is 5 μs.

comparable to decay length of the evanescent field some of the incident light is no longer totally internally reflected and I_r decreases; thus, a faint ring is observed as the impact dynamics begin, at $t = 11$ μs. In this case the fluid is not actually wetting the surface; instead the drop is supported by a thin layer of air. When wetting finally occurs, there is no longer any totally internally reflected light and a dark ring is observed, at $t = 22$ μs. As the drop continues to impinge on the surface the ring of wetting fluid grows both in the outward and inward directions, as shown for $t = 33$ μs.

To elucidate the impact dynamics we explore the behavior of drops falling from different initial heights. For $H = 1$ cm, we first detect the drop when a thin ring appears with an inner diameter of about 500 μm, as shown in Fig. 2(a)(i). The outer dimension of the ring grows rapidly as the drop falls, with an outward velocity of $\sim$1 m/s, comparable to the impact velocity of 0.44 m/s, as shown in Fig. 2(a)(ii). However, the fluid does not actually contact the surface; instead, the fluid spreads on a film of air only $\sim$100 nm thick. To visualize the dynamics we take a cut through the image at the location shown by the dashed red line in Fig. 2(a)(ii), convert the measured intensity to separation, and plot the time evolution, using color to denote the height, as shown in the 2D graph in Fig. 2(b). The first 500 μm clearly show the formation of the layer of air as the drop spreads before the liquid contacts the surface. The liquid does not spread inward, as seen by the boundaries of the thin film, denoted by the central region; this reflects the pocket of air which ultimately becomes a bubble trapped in the drop.

While the layer of air is clearly responsible for decelerating the drop, it cannot retain the separation of the fluid and surface indefinitely; ultimately, the thin film of air becomes unstable and contact occurs. Initially, two small dark spots appear in the film when the liquid fully contacts the surface, as shown in Fig. 2(a)(iii). These are denoted by the dark blue region at $t \sim 0.8$ ms in Fig. 2(b). As these spots grow, other spots appear, as the film of air breaks down, as shown in Fig. 2(a)(iv). These liquid wetting fronts spread rapidly, wetting the surface at a velocity of 1.5 m/s, comparable to that of the liquid spreading on the thin film of air. Interestingly, there is a thin line of air at the front of the spreading fluid where the air film becomes thicker as the air is pushed by the advancing wetting front, as shown by the white region leading the edge of the black wetting front. Ultimately two small air bubbles remain, displaced from the center of the drop, as shown by the arrows in Fig. 2(a)(vi) and Fig. 2(b).

Similar dynamics persist as the initial height of the drop is increased: the drop is again decelerated by a thin annulus of air with a thicker pocket in the middle; however, the thickness of the film of air also decreases, becoming of order 10 nm for a drop height of 4 cm. As H increases the initial size of the inner air pocket also decreases; moreover, the time during which its size remains constant is also reduced. Similarly, the thin film of air is only clearly observed over a much smaller region, prior to complete contact. For example, for $H = 3$ cm, the air film is $\sim$20 nm thick and is already only partly observed at the outer edges of the annulus, as shown by the 2D graph and confirmed by the snapshot [Fig. 2(c)]. As we increase the initial drop height to 4 cm, contact appears to occur around the full ring more rapidly than our frame rate of 60 kHz; however, even here the initial wetting is discontinuous, occurring in numerous discrete points as indicated by the rough texture of the inside of the ring. Thus, the drop is decelerated by an even thinner film which then breaks up at

discrete locations. As we increase H above 4 cm, we no longer have sufficient temporal resolution to routinely observe the initial film of air as it exists for a time that is short compared to the interframe time of the camera. Serendipitously, on rare occasions, the timing is exactly right that the camera captures the air film during the 1 μs exposure time even at H as high as 21 cm, confirming the existence of the air film at these larger heights.

To overcome this inherent limitation imposed by even the highest speed camera, we introduce a new imaging method, exploiting the fact that the intensity will change from completely bright to completely dark for a very small change in the liquid-solid separation. We exploit this nearly binary contrast by increasing the camera exposure time to integrate over times longer than the characteristic dynamics. This is illustrated schematically for a wetting front moving in one dimension in Fig. 3(a), using a composite image, which reflects the sum of the individual images at each time. The overexposed image displays a linear black to white gradient; this is essentially the sum of a series of individual virtual frames, which can be recovered by taking consecutive thresholds. We therefore call this method the virtual frame technique (VFT). The temporal resolution is determined by the dynamic range of the camera; thus, using a camera with 14-bit dynamic range, and an exposure time of 100 μs the VFT would allow us to resolve dynamics as short as 6 ns. For specific imaging sensors [17], this temporal resolution can be further improved by exploiting the gamma correction, which provides the camera an optional nonlinear integration time, and is particularly useful for isolating dynamics of accelerating fronts. Moreover, with VFT, the full spatial resolution of the camera is preserved. Thus, the VFT provides a combination of spatial and temporal resolution that is much greater than for any camera available [18].

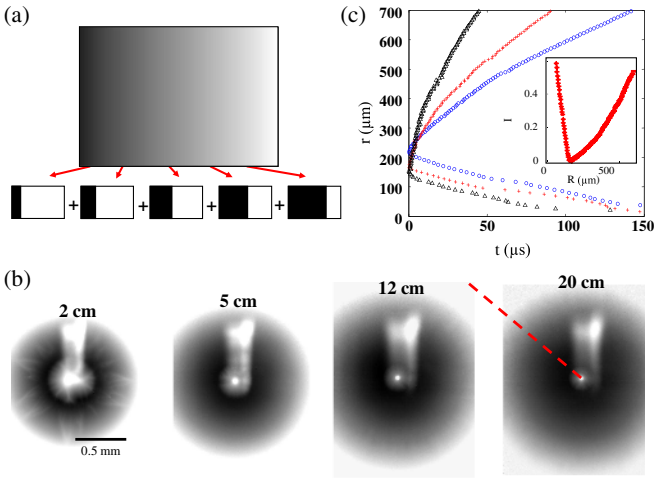

FIG. 3 (color online). Virtual frame technique (VFT). (a) 1D schematic demonstrating the concept. Individual binary images, below, are integrated to yield the total gray-scale image. The gray scale can be interpreted to yield the time evolution. (b) Four VFT images taken at different values of H. Each image exhibits a square-shaped whiter region through the top center resulting from spurious reflections in the beam path; they are ignored in our analysis. (c) The intensity is converted to time and azimuthally averaged around the impact center. The distance of the wetting fronts from the center are plotted as a function of time for three typical experiments with $H = 26, 126, 456$ mm for blue circles, red pluses and black triangles, respectively.

We employ the VFT to study the impact dynamics of drops released from initial heights ranging from 1 to 50 cm. For all H, the integrated image is disk shaped with a darker ring where contact first occurs, a bright white spot in the middle where the air bubble remains, and an evolution from black to gray to white moving outward where wetting has not yet occurred, as shown in Fig. 3(b). For $H = 2$ cm there are pronounced features in the image which are not observed for larger values of H, where the images are more symmetric. These features reflect the nonuniform nature of the initial wetting, consistent with the images in Fig. 2(c).

To quantify the VFT data, we measure intensity as a function of radial distance along the dashed line shown in Fig. 3(b), and plot the results in the inset of Fig. 3(c). The intensity data are converted to time to obtain the temporal evolution of the front, which is shown for several values of H in Fig. 3(c). The lower branch of each curve reflects the inward-traveling front as the ring closes to entrap the bubble in the middle of the drop; the upper branch of each curve reflects the outward-traveling front as the falling drop spreads. The point where the two meet is the radial distance at which contact first occurs, R_0; this is a decreasing function of initial height, as shown in Fig. 4(a), and the radial contact disc size exhibits a power-law dependence on H, with an exponent of $1/6$, consistent with theoretical predictions [1,18], as shown in the inset.

To explore the initial dynamics of the wetting associated with the rupture or breakdown of the air cushion, we numerically calculate the local instantaneous velocity and plot its magnitude as a function of radial position r. The inward-moving velocity is constant, propagating at approximately 1.3 m/s; by contrast, the outward-moving velocity decreases as $1/r$, and can exhibit remarkably high values, as large as $\sim$70 m/s, as shown in Fig. 4(b). Surprisingly, the velocity of the inward-moving front is independent of H; by contrast the maximum velocity of the outward-moving front increases strongly with H, as shown in Fig. 4(c). Moreover, the maximum velocity of the outward-moving front is nearly an order of magnitude greater than the capillary velocity for IPA, $\gamma/\mu \approx 10$ m/s.

When a contact line advances, it must flow on very small scales to maintain contact with the interface; flow on these small scales is dominated by viscous dissipation and thus, the propagation rates are limited by the liquid capillary velocity. By contrast, the velocities measured here are much larger; this suggests that the fluid is not in contact with the surface but is instead spreading on a thin film of

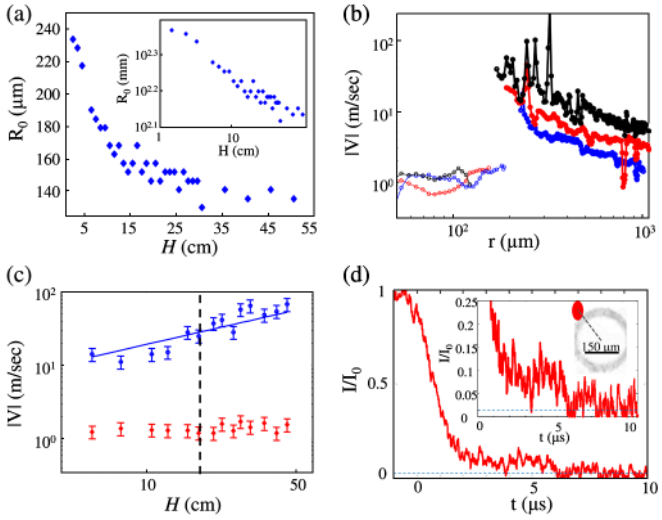

FIG. 4 (color online). The initial dynamics of the wetting. (a) R_0, as a function of H (inset) same as main figure in log scale. (b) The inward (solid circles) and outward (open circles) velocity of the spreading liquid for $H = 26$, 126, 456 mm corresponding to blue, red, and black, respectively. (c) Peak velocities for the outward (blue circles) and inward (red circles) fronts. Blue curve is the theoretically predicted initial outward spreading velocity [18]. The dashed line indicates the threshold height above which splashing is observed. (d) A photodiode trace acquired at 100 MHz measuring the intensity of the reflected light directly underneath the thin air film at a location marked by a red spot in the inset, for $H = 21$ cm. The dashed blue line marks the measurement noise floor. (inset) Closeup of the low intensity region. The image shown is a direct visualization of the thin film of air separating the liquid from the surface prior to contact.

air. Thus, the very early viscous dissipation is in the gas as it is squeezed out from under the liquid that wets the surface at an accelerated rate. Indeed, such high velocities are predicted theoretically [18], but only with the explicit assumption that the spreading occurs over a film of air, as indicated by the excellent agreement between the calculated behavior, shown by the solid line, and the data in Fig. 4(c). Although the VFT assumes nearly binary data, the resulting virtual frames will be practically indistinguishable for a simple dry-wet transition and an extremely short lasting air film which is followed immediately by a wetting front. To monitor the thin film of air for $H = 21$ cm, we measure the intensity using a photodiode operating at 100 MHz. The photodiode detects an area $\sim 2500\ \mu m^2$; by comparison, the thin film of air is initially about 200 μm in diameter, as shown by the camera image in the inset to Fig. 4(d). We normalize the photodiode intensity to that obtained before the drop hits the interface, I_0. The intensity initially drops rapidly, corresponding to the passage of the liquid over the area sampled by the photodiode; the steep slope of the intensity drop is indicative of the very high speed at which the liquid spreads. However, the intensity does not drop all the way to zero, but instead levels off, reaching a plateau at a value $I/I_0 \sim 0.1$, and finally decreasing to zero after ~ 5 μs as shown in the enlarged data in the inset of Fig. 4(d). This plateau directly reflects the existence of the thin film of air that separates the liquid from the surface. The nature of the final decay of this plateau differs from experiment to experiment, as shown, for example, in the Supplemental Information [18] Fig. S2(ii). This reflects the specific dynamics of the dewetting of the air film, which can vary due to the specific spinodal decomposition that occurs in each case. These measurements directly confirm the spreading of the liquid on a thin film of air of order 10 nm thick; this is trailed closely by a wetting front that rapidly expands due to the breakdown of the air film.

Our results directly demonstrate the existence of a thin film of air over which the liquid spreads; this provides striking confirmation of the theoretical prediction [1,13]. In addition, our results reveal that qualitatively new phenomena occur as the thin film of air becomes unstable, simultaneously breaking down at many discrete locations, leading to wetting patches that grow and coalesce to fully wet the surface. Similar dynamics have also been reported to occur when a sheet of fluid is ejected as a drops splash after high velocity impact [11,19]. For a perfectly wetting fluid such as IPA on glass, a thin film of air behaves as does a poor solvent; it cannot remain stable and van der Waals forces will cause it to dewet the surface through a nucleation or spinodal-like process [20,21]; indeed Fig. 2(a)(ii) is reminiscent of the patterns observed in such processes. Dewetting dynamics are traditionally considered to be quite slow [20,21]; however, for spinodal dewetting the rate of film breakup depends strongly on its thickness [21] and also on viscosity and may occur very rapidly; for example, a 10 nm thick air film will remain stable for no longer than 1 μs. Thus, rupturing occurs simultaneously at many discrete locations; this leads to small wetting patches that grow and coalesce to fully cover the surface, thereby very rapidly following the advancing fluid front. This gives the appearance of a single contact line moving at the same velocity as the fluid, much faster than the calculated capillary velocity.

Using a novel experimental modality that visualizes the falling drop from below rather than from the side, we identify a thin film of air that initially separates the liquid from the surface. Eventually, however, spinodal-like dewetting of the air film always leads to its breakup and complete contact of the surface by the fluid. The rate at which contact occurs depends on the rate of this spinodal-like process, which depends on the thickness of the air film. Initially, as H is increased, the air film becomes thinner, and the breakup of the air film occurs more rapidly; thus, even though the rate of initial drop spreading increases with H, the length over which the drop skates on the air film decreases. However, as H increases still further, the thickness of the air film saturates, and hence the rate of

breakup also saturates; however, the rate of initial spreading of the drop continues to increase with H. Thus, the drop always can skate over the film of air, even as H continues to increase. Interestingly, this skating on the film of air can persist, even until H increases enough that a sheet of fluid is ejected near the expanding rim, and a splash is produced. This suggests that dynamics of this ephemeral film of air may be of far greater importance, and may in fact influence splashing; however, confirmation of this speculation requires further investigation.

This work was supported by the NSF (DMR-10006546) and the Harvard MRSEC (DMR-0820484), and the Harvard Kavli Institute for Bio-nano-science and Technology. J. M. K. acknowledges the support from the NDSEG Fellowship. S. M. R. acknowledges the support from the Yad Hanadiv Rothschild Foundation. L. M. acknowledges support from the MacArthur Foundation.

*shmuel.rubinstein@weizmann.ac.il

[1] M. Mani, S. Mandre, and M. P. Brenner, J. Fluid Mech. **647**, 163 (2010).
[2] A. L. Yarin, Annu. Rev. Fluid Mech. **38**, 159 (2006).
[3] L. Courbin, J. C. Bird, M. Reyssat, and H. A. Stone, J. Phys. Condens. Matter **21**, 464127 (2009).
[4] R. D. Schroll, C. Josserand, S. Zaleski, and W. W. Zhang, Phys. Rev. Lett. **104**, 034504 (2010).
[5] J. C. Bird, S. Mandre, and H. A. Stone, Phys. Rev. Lett. **100**, 234501 (2008).
[6] A. M. Worthington, Proc. R. Soc. London **25**, 261 (1876).
[7] C. Josserand, L. Lemoyne, R. Troeger, and S. Zaleski, J. Fluid Mech. **524**, 47 (2005).
[8] M. B. Lesser, Proc. R. Soc. A **377**, 289 (1981).
[9] M. B. Lesser and J. E. Field, Annu. Rev. Fluid Mech. **15**, 97 (1983).
[10] L. Xu, W. W. Zhang, and S. R. Nagel, Phys. Rev. Lett. **94**, 184505 (2005).
[11] M. M. Driscoll, C. S. Stevens, and S. R. Nagel, Phys. Rev. E **82**, 036302 (2010).
[12] M. Rein and J. P. Delplanque, Acta Mech. **201**, 105 (2008).
[13] S. Mandre, M. Mani, and M. P. Brenner, Phys. Rev. Lett. **102**, 134502 (2009).
[14] S. T. Thoroddsen, T. G. Etoh, K. Takehara, N. Ootsuka, and Y. Hatsuki, J. Fluid Mech. **545**, 203 (2005).
[15] M. M. Driscoll and S. R. Nagel, Phys. Rev. Lett. **107**, 154502 (2011).
[16] S. M. Rubinstein, G. Cohen, and J. Fineberg, Nature (London) **430**, 1005 (2004).
[17] S. Ham, W. Jung, S. Lim, Y. Lee, and G. Han, Jpn. J. Appl. Phys. **45**, 2522 (2006).
[18] See Supplemental Material at http://link.aps.org/supplemental/10.1103/PhysRevLett.108.074503 for a detailed description of the experimental methods and additional photodiode measurements.
[19] S. T. Thoroddsen, K. Takehara, and T. G. Etoh, Phys. Fluids **22**, 051701 (2010).
[20] G. Reiter, Phys. Rev. Lett. **68**, 75 (1992).
[21] P. G. De Gennes, F. Brochard-Wyart, and D. Quéré, *Capillarity and Wetting Phenomena: Drops, Bubbles, Pearls, Waves* (Springer Verlag, New York, 2004).